RESEARCH ARTICLE | MARCH 05 2024

The approximate coupled-cluster methods CC2 and CC3 in a finite magnetic field

Marios-Petros Kitsaras ; Laura Grazioli ; Stella Stopkowicz

J. Chem. Phys. 160, 094112 (2024)
https://doi.org/10.1063/5.0189350

The Journal of Chemical Physics ARTICLE pubs.aip.org/aip/jcp

The approximate coupled-cluster methods CC2 and CC3 in a finite magnetic field

Cite as: J. Chem. Phys. 160, 094112 (2024); doi: 10.1063/5.0189350
Submitted: 28 November 2023 • Accepted: 18 January 2024 •
Published Online: 5 March 2024 • Publisher Error Corrected: 31 July 2024

Marios-Petros Kitsaras,[1,2,a] Laura Grazioli,[2,b] and Stella Stopkowicz[1,2,3,c]

AFFILIATIONS

[1] Fachrichtung Chemie, Universität des Saarlandes, Campus B2.2, D-66123 Saarbrücken, Germany
[2] Department Chemie, Johannes Gutenberg-Universität Mainz, Duesbergweg 10-14, D-55128 Mainz, Germany
[3] Hylleraas Centre for Quantum Molecular Sciences, Department of Chemistry, University of Oslo, P.O. Box 1033 Blindern, N-0315 Oslo, Norway

[a] **Electronic mail:** marios.kitsaras@uni-saarland.de
[b] **Electronic mail:** lgraziol@uni-mainz.de
[c] **Author to whom correspondence should be addressed:** stella.stopkowicz@uni-saarland.de

ABSTRACT

In this paper, we report on the implementation of CC2 and CC3 in the context of molecules in finite magnetic fields. The methods are applied to the investigation of atoms and molecules through spectroscopic predictions and geometry optimizations for the study of the atmosphere of highly magnetized White Dwarf stars. We show that ground-state finite-field (ff) CC2 is a reasonable alternative to CCSD for energies and, in particular, for geometrical properties. For excited states, ff-CC2 is shown to perform well for states with predominant single-excitation character. Yet, for cases in which the excited state wavefunction has double-excitation character with respect to the reference, ff-CC2 can easily lead to completely unphysical results. Ff-CC3, however, is shown to reproduce the CCSDT behavior very well and enables the treatment of larger systems at a high accuracy.

I. INTRODUCTION

In recent decades, the chemistry in extreme environments has increased significantly as an active area of research.[1–9] Studies of atoms and molecules in strong magnetic fields began already in the 1980s and 1990s [10–15] and the interest was revitalized in the 2000s for the study of molecular magnetic properties as well as molecules in magnetic fields with an arbitrary strength and orientation.[16–29] Theoretical investigation of molecules in magnetic fields that are unattainable experimentally attracts special interest as it enables, for example, the study of the atmospheres of magnetic White Dwarf (WD) stars. The magnetic field on these celestial objects can be strong enough to compete with Coulomb interactions.[30–34] The study of WDs aims to achieve a deeper understanding of the life cycle of stars and evolution of the universe in general.[10,15,30–44] The additional fact that in the atmospheres of WD stars molecules are observed[44] offers a unique opportunity to study the exotic chemistry that arises when the magnetic interaction is at the same order of magnitude as the Coulomb interaction.[7] Concerning quantum-chemical studies for such systems, both the magnetic and Coulomb interaction need to be treated with non-perturbative quantum-chemical methods. These so-called finite-field (ff) methods require the use of complex algebra and deal with the gauge-origin dependence in the Hamiltonian. The use of complex algebra increases the computational cost, due to the need to handle complex rather than real values, and matrix multiplication is 3–4 times slower as compared to the real case.[45] Nowadays, gauge including atomic orbitals (GIAOs) also known as London orbitals[46] are typically employed to ensure gauge-origin independent results.[17] Implementations of different ff-methods in quantum-chemical programs that can handle arbitrarily oriented magnetic fields have been carried out in various program packages.[25,47–54]

Strong magnetic fields alter chemistry in such a way that common chemical intuition is no longer applicable. The combination of competing paramagnetic and diamagnetic influences may alter the ground state of atoms and molecules.[21] Unusual phenomena, like perpendicular paramagnetic bonding,[7] may also take place. Ff-coupled-cluster (CC) methods[55] are a valuable tool to study this

complex behavior, since they give highly accurate results with a clear way for systematic improvement.[21] In addition, excited states may be studied by the ff-variants of equation of motion (EOM)-CC theory.[21,22,56–58]

The most common CC variant used is probably "CC singles and doubles" (CCSD) theory. This method can be used for states described well by a single determinant and is applicable for small- to medium-sized molecules.[59] Regarding larger molecules, its use is limited due to the unfavorable N^6 scaling, with N being the system size. In ff-calculations, the formal scaling is identical albeit with a larger prefactor. Molecular symmetry may be exploited using group theory to moderate the computational demands even in ff-calculations,[60–62] though the symmetry is typically reduced by the magnetic field.[63–65] Additionally, approaches that aim to lower the computational cost by approximating the four-center two-electron integrals like the Cholesky Decomposition (CD)[28,66–68] or the Resolution of the Identity (RI)[26,69] have merit in combination with ff-CC methods, though they do not lower the overall scaling in CC calculations. Another way to moderate the cost of standard CC truncations is by approximating the amplitude equations. Such an approximation is offered by the CCn series of methods that lower the scaling of the parent method and are based on perturbation theory.[70–73]

CC2 is an approximation to CCSD and provides a lower scaling while often retaining a similar accuracy for energy differences.[70] The method is used exceedingly either to study larger molecules or to benchmark results from more approximate methods when CCSD is too expensive.[74–84] The approximate CC2 method scales similarly to MP2, i.e., with N^5, but, due to the inclusion of single excitations acting like an approximate orbital response, gives results of higher quality, especially for properties.[70,85,86] Accordingly, spin contamination at the CC2 level is significantly reduced compared to MP2.[87] An essential feature of CC2 is that, unlike MP2, it can be rigorously extended to target excited states (EOM-CC2), thus enabling their treatment in larger systems at the CC level.

In certain applications, an accuracy beyond CCSD may be needed. This is for example the case in studies of systems with moderate static-correlation character or excited states with a significant double-excitation character with respect to the reference. Since the next-higher-order truncation, "CC singles doubles and triples" CCSDT, scales as N^8, its applicability is limited significantly. For ground states, the approximate triples scheme CCSD(T) is considered the "gold standard".[88] Only one non-iterative N^7 step is needed here, but the extension to excited states is not straightforward. Moreover, the method is known to be sensitive to spin contamination.[89] The approximate inclusion of triple corrections via the CC3 model scales as N^7 as well, though iteratively, and is easily generalized to the EOM approach for treatment of excited states.[71–73] Recently, numerous applications of the CC3 approach have been reported: Highly accurate results at the CC3 level of theory are used for comparison with more approximate methods[90] and interpretation of experimental data (e.g., UV spectroscopy, x-ray spectroscopy, organic photochemistry).[91–97] CC3 has also contributed to the creation of databases and benchmarks for the electronic-structure community.[98–100] Recent work toward more efficient implementations of CC3 for closed-shell systems by Paul, Myhre, and Koch has allowed applications to larger systems with more than 500 basis functions.[73] In the context of ff-methods, highly accurate results beyond CCSD are needed, for example, for the prediction and assignment of absorption spectra from magnetic WD stars.[58] Additionally, when increasing the magnetic-field strength, double-excitation character can be transferred back and forth between various states.[58] The resulting problem of a deteriorating quality in the accuracy of predictions can be dealt with by inclusion of triple excitations, as shown in a study at the ff-CCSDT level.[58] Hence, the ff-CC3 model, as is often the case for calculations in the absence of a magnetic field, may prove very useful to treat systems where the full ff-CCSDT method is not feasible.

In this paper, the implementation of ff-CC2 and ff-CC3 methods is reported. It is based on a spin-unrestricted formulation that is able to target open-shell systems. Open-shell electronic configurations are typically stabilized in a magnetic field because of the spin-Zeeman influence and become ground states in stronger fields. In Sec. II, the theoretical aspects of CCn approximations are briefly presented as well as their extensions to EOM-CC theory.[70–73] Details on the implementation are discussed in Sec. III. We note that ff-CC2 has been reported recently in the literature in terms of benchmark data,[27] but no dedicated implementation or investigation of its performance has been presented. Finally, applications of ff-CC2 and ff-CC3 are presented in Sec. IV. These include an investigation of the excitation spectrum of the Mg atom in the presence of a strong magnetic field, calculations on the diatomic cation CH^+ and the CH radical, and geometry optimization in the presence of a magnetic field for methane CH_4 and ethylene CH_2CH_2.

II. THEORY

A. Molecular Hamiltonian in the presence of a magnetic field

The electronic Hamiltonian for a molecule in the presence of a uniform magnetic field $\boldsymbol{B}$ is given in atomic units by

$$\hat{H} = \hat{H}_0 + \sum_i \left(\frac{1}{2}\boldsymbol{B}\cdot\hat{\boldsymbol{l}}_i^O + \boldsymbol{B}\cdot\hat{\boldsymbol{s}}_i \right) + \sum_i \frac{1}{8}\left(\boldsymbol{B}^2\boldsymbol{r}_{Oi}^2 - |\boldsymbol{B}\cdot\boldsymbol{r}_{Oi}|^2 \right). \quad (1)$$

In the equation above, $\hat{H}_0$ is the field-free electronic molecular Hamiltonian. The additional terms involve the angular momentum operator $\hat{\boldsymbol{l}}_i^O$ around a gauge origin O, the electron-spin operator $\hat{\boldsymbol{s}}_i$, and the position operator $\boldsymbol{r}_{Oi}$ with respect to the gauge origin.[12]

A change of the gauge origin $O \to O'$ results in a phase oscillation for exact wavefunctions $\Psi^{O'} = e^{-if}\Psi^O$. Expectation values thus remain gauge-origin invariant $\langle\Psi^{O'}|\hat{A}|\Psi^{O'}\rangle = \langle\Psi^O|\hat{A}|\Psi^O\rangle$. To obtain gauge-origin independent results in the case of approximate wavefunctions, gauge including atomic orbitals, also called London orbitals, may be employed

$$\omega_\mu(\boldsymbol{B}, \boldsymbol{r}_A, \boldsymbol{r}_O) = \mathrm{e}^{\frac{i}{2}\boldsymbol{B}\times(\boldsymbol{r}_O-\boldsymbol{r}_A)\cdot\boldsymbol{r}}\chi_\mu \quad (2)$$

with $\boldsymbol{r}_A$ being the position of the nuclear center of the atomic orbital and χ_μ the standard atomic orbital.[46]

The presence of the angular-momentum operator and the employment of London orbitals necessitate the use of complex algebra, which increases the computational demands.[45]

B. Coupled cluster theory

In the CC ansatz,[55] the wavefunction is written as the exponential of the cluster operator $\hat{T} = \sum_I \hat{T}_I = \sum_I t_I \hat{\mu}_I$ acting on a reference wavefunction $|0\rangle$, which is usually the Hartree–Fock (HF) solution[59]

$$|\mathrm{CC}\rangle = \mathrm{e}^{\hat{T}}|0\rangle. \tag{3}$$

The index I denotes the level of excitation, t_I are the cluster amplitudes, and $\hat{\mu}_I$ a string of quasiparticle creation operators that give the excited determinant $|\mu_I\rangle$ starting from the reference $|0\rangle$. Using the similarity-transformed Hamiltonian

$$\widetilde{H} = \mathrm{e}^{-\hat{T}}\hat{H}\mathrm{e}^{\hat{T}}, \tag{4}$$

the CC energy is given as

$$E_{\mathrm{CC}} = \langle 0|\widetilde{H}|0\rangle. \tag{5}$$

The equations that determine the cluster amplitudes t_I are the CC equations that require the projections on excited determinants $\langle\mu_I|$ to vanish,

$$0 = \langle\mu_I|\widetilde{H}|0\rangle. \tag{6}$$

Standard CC approximations truncate the cluster operator to a specific excitation level, e.g., for CCSD: $\hat{T} = \hat{T}_1 + \hat{T}_2$, for CCSDT: $\hat{T} = \hat{T}_1 + \hat{T}_2 + \hat{T}_3$, and so on, and the CC equations needed to determine the cluster amplitudes t_I only make use of excited determinants up to the same excitation level.

C. The equation of motion approach

In the EOM-CC approach, excited states are described by acting with a linear excitation operator $\hat{R} = \sum_I \hat{R}_I = \sum_I r_I \hat{\mu}_I$ on the CC wavefunction such that[56,59]

$$|\mathrm{EOM}\rangle = \hat{R}|\mathrm{CC}\rangle. \tag{7}$$

The determination of EOM amplitudes r_I^k is achieved by solving the energy eigenvalue problem and results in the expression

$$\langle\nu_J|\left[\widetilde{H}, \hat{R}^k\right]|0\rangle = \omega^k_{\mathrm{exc}}\langle\nu_J|\hat{R}^k|0\rangle, \tag{8}$$

$$\sum_I \langle\nu_J|\left[\widetilde{H}, \hat{\mu}_I\right]|0\rangle r_I^k = \omega^k_{\mathrm{exc}} r_J^k. \tag{9}$$

The EOM thus defines a CI-like eigenvalue problem, with r_I^k being the k-th right-eigenvector solution, and $\omega^k_{\mathrm{exc}} = E^k_{\mathrm{exc}} - E_{\mathrm{CC}}$ its eigenvalue. Usually, the $\hat{R}$ operator is truncated at the same level as the CC truncation it is based on. The matrix elements $\langle\nu_K|\left[\widetilde{H}, \hat{\mu}_I\right]|0\rangle$ form the connected contributions to the CC Jacobian matrix, which can be viewed as the gradient of the CC Lagrangian with respect to t_I amplitudes.[56] This "connectedness" is the result of using the commutator $\left[\widetilde{H}, \hat{\mu}_I\right]$ for the derivation of working equations. It ensures that only contributions that involve contractions between the Hamiltonian and the excitation operator in a diagrammatic sense contribute, which results in size-intensive energies.[59]

The non-Hermiticity of the similarity-transformed Hamiltonian $\widetilde{H}$ may result in nonphysical complex energy eigenvalues for both the ground and excited states at the truncated CC level of theory. While this issue is usually not prominent in the field-free case except in the vicinity of conical intersections,[101] complex eigenvalues often occur in ff-CC calculations. This behavior has been investigated in Ref. 102. Usually, the imaginary part is well below the chemical accuracy ($<10^{-3}$ E_h) and is reduced when including higher-order correlation treatment. Formally, unitary CC approaches, like UCCn, or algebraic diagrammatic construction (ADCn) remedy this nonphysical behavior.[103,104] Work along these lines is currently being pursued.[105]

D. The CCn approximation

The CCn series introduced in the work of Christiansen *et al.*[70–73] aims to approximate the standard CC truncations with a more favorable scaling. This series of approximations is based on the perturbation expansion of the CC energy and the Møller–Plesset (MP)[106] partitioning of the Hamiltonian

$$\hat{H} = \hat{F} + \hat{V}. \tag{10}$$

Here, the zeroth-order Hamiltonian corresponds to the sum of Fock operators $\hat{F} = \sum_\alpha \hat{f}(\alpha)$ and the fluctuation potential $\hat{V} = \hat{H} - \hat{F}$ is the perturbation. Unlike many-body perturbation theory (MBPT),[59] the CCn series has two requirements:[70,72]

1. The singles amplitudes t_1 are treated in zeroth order, as they function as effective orbital relaxation.
2. The amplitude equations of excitation level n, where n is the cardinal number of the method, are simplified till the first nonvanishing order.

With the help of partially transformed operators

$$\bar{O} = \mathrm{e}^{-\hat{T}_1}\hat{O}\mathrm{e}^{\hat{T}_1}, \tag{11}$$

it is ensured that contributions of $\hat{T}_1$ will be included up to infinite order of perturbation.

In the singles approximate doubles model, CC2,[70] the double amplitude equations are truncated up to first order as dictated by the second requirement

$$0 = \langle\mu_2|\bar{V} + \left[\bar{F}, \hat{T}_2\right]|0\rangle. \tag{12}$$

Assuming the occupied–occupied and virtual–virtual blocks of the Fock matrix to be diagonal results in

$$0 = \langle\mu_2|\bar{V}|0\rangle + \Delta\varepsilon_2 t_2, \tag{13}$$

$$t_2 = -\frac{\langle\mu_2|\bar{V}|0\rangle}{\Delta\varepsilon_2}, \tag{14}$$

where $\Delta\varepsilon_2$ signifies the orbital-energy differences $\varepsilon_a + \varepsilon_b - \varepsilon_i - \varepsilon_j$. In the notation used $a, b, c, \ldots$ signify virtual orbitals and $i, j, k, \ldots$ occupied orbitals. For the singles doubles approximate triples model, CC3,[72] one simplifies the triples amplitude equations till second order such that

$$0 = \langle \mu_3 | \left[\bar{V}, \hat{T}_2 \right] + \left[\bar{F}, \hat{T}_3 \right] | 0 \rangle, \tag{15}$$

$$t_3 = -\frac{\langle \mu_3 | \left[\bar{V}, \hat{T}_2 \right] | 0 \rangle}{\Delta\varepsilon_3}. \tag{16}$$

Again, canonical or semi-canonical orbitals are assumed. $\Delta\varepsilon_3$ is the orbital-energy difference $\varepsilon_a + \varepsilon_b + \varepsilon_c - \varepsilon_i - \varepsilon_j - \varepsilon_k$.

Building the CCn Jacobian to form the EOM eigenvalue problem results in

$$\begin{pmatrix} \langle \nu_1 | \left[\bar{H}, \hat{\mu}_1 \right] + \left[\left[\bar{H}, \hat{\mu}_1 \right], \hat{T}_2 \right] | 0 \rangle & \langle \nu_1 | \left[\bar{H}, \hat{\mu}_2 \right] | 0 \rangle \\ \langle \nu_2 | \left[\bar{V}, \hat{\mu}_1 \right] | 0 \rangle & \langle \nu_2 | \left[\hat{F}, \hat{\mu}_2 \right] | 0 \rangle \end{pmatrix} \begin{pmatrix} r_1 \\ r_2 \end{pmatrix} = \omega_{\text{exc}} \begin{pmatrix} r_1 \\ r_2 \end{pmatrix} \tag{17}$$

for EOM-CC2[70] and

$$\begin{pmatrix} \langle \nu_1 | \left[\bar{H}, \hat{\mu}_1 \right] + \left[\left[\bar{H}, \hat{\mu}_1 \right], \hat{T}_2 \right] | 0 \rangle & \langle \nu_1 | \left[\bar{H}, \hat{\mu}_2 \right] | 0 \rangle & \langle \nu_1 | \left[\hat{H}, \hat{\mu}_3 \right] | 0 \rangle \\ \langle \nu_2 | \left[\bar{H}, \hat{\mu}_1 \right] + \left[\left[\bar{H}, \hat{\mu}_1 \right], \hat{T}_2 + \hat{T}_3 \right] | 0 \rangle & \langle \nu_2 | \left[\bar{H}, \hat{\mu}_2 \right] + \left[\left[\bar{H}, \hat{T}_2 \right], \hat{\mu}_2 \right] | 0 \rangle & \langle \nu_2 | \left[\bar{H}, \hat{\mu}_3 \right] | 0 \rangle \\ \langle \nu_3 | \left[\left[\bar{V}, \hat{\mu}_1 \right], \hat{T}_2 \right] | 0 \rangle & \langle \nu_3 | \left[\bar{V}, \hat{\mu}_2 \right] | 0 \rangle & \langle \nu_3 | \left[\hat{F}, \hat{\mu}_3 \right] | 0 \rangle \end{pmatrix} \begin{pmatrix} r_1 \\ r_2 \\ r_3 \end{pmatrix} = \omega_{\text{exc}} \begin{pmatrix} r_1 \\ r_2 \\ r_3 \end{pmatrix} \tag{18}$$

for EOM-CC3.[71,73]

Noting that within EOM-CC2, double-excitation amplitudes r_2 are fully determined by the singles amplitudes r_1 (see also Sec. III A), one could rewrite the EOM-CC2 eigenvalue problem as a nonlinear set of equations involving only r_1 amplitudes. For those cases in which the doubles amplitudes are the *leading* contributions for the excited state, the approximation breaks down, meaning that states with a predominant double-excitation character cannot be targeted by the EOM-CC2 approach.[70] The same is in principle true for CC3 and excited states with predominant triple-excitation character, but such states are of no particular concern in practical applications.

III. IMPLEMENTATION

The implementation of ff-CC2 and ff-CC3 as well as the EOM approach of these methods has been carried out in the QCUMBRE program package.[22,47]

A. General considerations

The scaling of the (EOM-)CC2 and (EOM-)CC3 methods is N^5 and N^7, respectively, which is one order of magnitude less than their parent methods CCSD and CCSDT. Beyond this reduction in computational cost, an efficient implementation can be achieved, when using canonical or semi-canonical orbitals. The diagonal form of the Fock matrix results in a diagonal form of the n-th amplitudes equations. Hence, doubles amplitudes can be expressed as a function of the singles amplitudes alone with no doubles to doubles contributions for CC2 [see Eq. (14)]. Similarly for CC3, the triples amplitudes equations can be brought into a form that depends only on the singles and doubles with no triples to triples contributions [see Eq. (16)]. This commonly used approach allows for an *on-the-fly* calculation of the amplitudes with reduced memory requirements.[107]

Turning to Jacobian matrices, similar equations have been derived for the approximated r_n amplitudes for excited states, where n is the cardinal number of the method. Starting from the last row of Eq. (17), the expression

$$\langle \nu_2 | \left[\bar{V}, \hat{\mu}_1 \right] | 0 \rangle r_1 + \Delta\varepsilon_2 r_2 = \omega_{\text{exc}} r_2, \tag{19}$$

$$\frac{\langle \nu_2 | \left[\bar{V}, \hat{\mu}_1 \right] | 0 \rangle r_1}{\omega_{\text{exc}} - \Delta\varepsilon_2} = r_2 \tag{20}$$

is obtained for CC2. Similarly, continuing from the last row of Eq. (18) leads to the diagonal r_3 elements of EOM-CC3,

$$\langle \nu_3 | \left[\left[\bar{V}, \hat{\mu}_1 \right], \hat{T}_2 \right] | 0 \rangle r_1 + \langle \nu_3 | \left[\bar{V}, \hat{\mu}_2 \right] | 0 \rangle r_2 + \Delta\varepsilon_3 r_3 = \omega_{\text{exc}} r_3, \tag{21}$$

$$\frac{\langle \nu_3 | \left[\left[\bar{V}, \hat{\mu}_1 \right], \hat{T}_2 \right] | 0 \rangle r_1 + \langle \nu_3 | \left[\bar{V}, \hat{\mu}_2 \right] | 0 \rangle r_2}{\omega_{\text{exc}} - \Delta\varepsilon_3} = r_3. \tag{22}$$

Equations (20) and (22) show, similar to the ground state treatment, that the r_n amplitudes of EOM-CCn can be fully determined by the lower excitation levels and can thus be considered redundant information not to be saved in memory. Unlike the t_n amplitudes, however, they require the calculation of the exact excitation energy, which is available only at convergence. It is well known and exploited in many field-free EOM-CCn implementations that to deal with this issue, the Davidson method in EOM-CCn calculations needs to be modified. Details on these modifications can be found in Ref. 65.

B. Validation

To verify the implementation, the code has been tested for the field-free case against calculations using the closed-shell implementation of the CFOUR program.[48,108] For calculations in a finite magnetic field and for the case of an unrestricted reference, the CCSD and CCSDT methods already implemented in QCUMBRE were modified to produce results at the (EOM-)CC2 and CC3 levels, respectively, to verify the more efficient CC2 and CC3 implementations.

IV. RESULTS AND DISCUSSION

All post-HF calculations were performed using the QCUMBRE program package.[47] QCUMBRE works together with an interface to the CFOUR program[48,108] that provides integrals over London orbitals via the MINT integral code[109] and a ff-UHF reference wavefunction.

First, the investigation of the Mg atom will be presented, followed by calculations on the CH^+ and CH molecules. An unrestricted approach is used for the open-shell systems. Lastly, the results for geometry optimizations for methane and ethylene in different magnetic fields will be presented. The discussion in the following paragraphs is centered on the performance of the CC2 and CC3 methods, while an investigation of the physical and chemical behavior of the systems in the presence of a magnetic field is presented in Ref. 65.

A. Atomic Mg

In the atmosphere of WDs, metals are often detected due to incoming material from planetary or asteroidal debris.[43,110,111] In the current study, highly accurate results for the Mg atom have been generated at the CC3 level of theory in order to investigate such contaminants in magnetic WDs. Specifically, transitions from the lowest triplet state ^3P_u described by electronic configuration $1s^2 2s^2 2p^6 3s^1 3p^1$ to triplet states ^3S_g ($1s^2 2s^2 2p^6 3s^1 4s^1$) and ^3D_g ($1s^2 2s^2 2p^6 3s^1 3d^1$) were investigated as they are expected to give strong signals.[112] The electronic states involved were studied at the CCSD and CC3 levels of theory using a series of uncontracted (unc) basis sets, namely the unc-aug-cc-pCVXZ sets,[113–116] with X being the cardinal number of the basis set. Using the unc-aug-cc-pCVTZ basis, additional calculations at the CCSDT level of theory were performed to benchmark the CC3 results. The magnitude of the triples corrections was calculated as the difference between the CCSDT and CCSD energy. Calculations were performed in the range of field strengths between $0.0B_0$ and $0.2B_0$. A dense spacing of $0.004B_0$ was used up to $0.1B_0$, continuing with a spacing of $0.02B_0$ for the last increment.

The results for total energies at various levels of theory are shown in Fig. 1. Following a similar strategy as in Ref. 58, an extrapolation scheme has been employed to generate accurate B-λ curves. In these curves, the magnetic-field strength is plotted as a function of the transition wavelength in Fig. 2. The extrapolation scheme used for the generation of accurate B-λ curves follows

$$\Delta E_{\mathrm{exc}}^{\mathrm{corrected}} = \Delta E_{\mathrm{exc}} + \Delta E_{\mathrm{basis}} + \Delta E_{\mathrm{triples}}. \tag{23}$$

For the extrapolation, the CCSD/unc-aug-cc-pV5Z results were used for the excitation energies ΔE_{exc} and the unc-aug-cc-pCVQZ and unc-aug-cc-pCV5Z basis sets for the basis set extrapolation contribution $\Delta E_{\mathrm{basis}}$.[58] Higher-order correlation was accounted for via triples corrections $\Delta E_{\mathrm{triples}} = E_{\mathrm{triples}} - E_{\mathrm{CCSD}}$ at the CC3/unc-aug-cc-pCVQZ levels of theory. Lastly, an offset correction relative to spin-averaged values from the NIST database[112] is added. The selection rule $\Delta M_L = 0, \pm 1$ (0 blue, +1 red, −1 green) was used to construct visible transitions. In the figure, the results of a simple perturbative Zeeman correction $E_{\mathrm{Zeeman}} = \frac{1}{2} M_L B$ were plotted as well (dotted curves). Deviation from this simple correction shows the importance of ff-quantum-chemical predictions for the assignment of spectra at high-field strengths.

As seen in Fig. 1, the CCSD energies (long dashed curves) are energetically slightly higher as compared to the CCSDT reference. In contrast, the CC3 results are practically identical to CCSDT and cannot be distinguished in the plot. The calculated deviation of approximate triples relative to the inclusion of full triples is at the order of only $10^{-5} E_{\mathrm{h}}$. The lower computational cost of CC3 compared to CCSDT and good agreement between these two methods enable an accurate treatment of triple excitations using larger basis sets that is not feasible with a full treatment of triples.

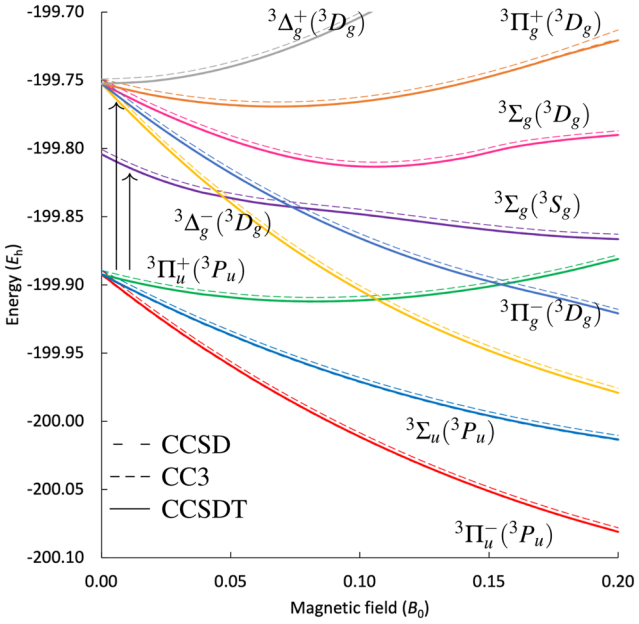

FIG. 1. Low-lying triplet states of Mg calculated at the EOM-CCSD, EOM-CC3, and EOM-CCSDT levels of theory using an unc-aug-cc-pCVTZ basis set.

It is important to note that the use of the CC3 method for the generation of extrapolated B-λ curves has allowed the use of triple corrections calculated with larger basis sets. The comparison with CCSDT results reveals the potential of CC3 to practically replicate the full inclusion of triples corrections for the electronic transitions studied. The states studied at the EOM-CC level of theory for this increment of magnetic-field strengths have predominantly single-excitation character. Only the $^3\Pi_g^+(^3D_g)$ state acquires a significant double-excitation character at the EOM-CC3 and EOM-CCSDT levels of theory for $B = 0.20B_0$.[117] This results in an increase in triple corrections as seen in Fig. 1 for the orange curve. Note that we provide the symmetry of the system within the magnetic field and in parentheses its symmetry in the field-free case. The double-excitation character arises from a mixing of the $^3\Pi_g^{\pm}(^3D_g)$ components with an energetically higher-lying $^3\Pi_g^{\pm}(^3P_g)$ state with predominant $1s^2 2s^2 2p^6 3p^2$ configurations. Moreover, the developments presented here contributed to the assignment of Mg in the spectrum of a magnetized WD,[118] which would have not been possible without ff-quantum-chemical predictions.

B. CH^+ and CH in varying magnetic fields

Calculations on the closed-shell methylidinium cation CH^+ and the open-shell CH radical have been carried out using a contracted and an unc-cc-pVDZ basis set, respectively. The CH radical has been detected in weakly magnetized WDs along with C_2.[31,44]

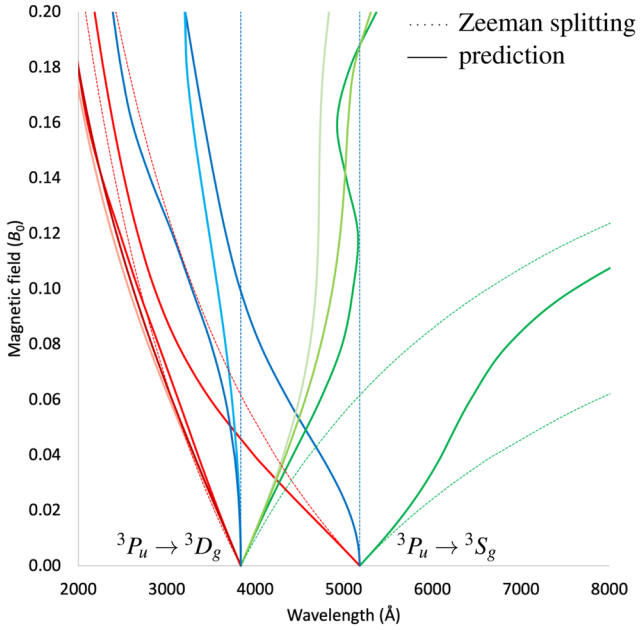

FIG. 2. Extrapolated B-λ curves for the $^3P_u \rightarrow {}^3S_g$ and $^3P_u \rightarrow {}^3D_g$ transitions of Mg. The $\Delta M_L = 0$ components are shown in blue, $\Delta M_L = +1$ in red, and $\Delta M_L = -1$ in green.

This is an indication that the radical or its cation may be present in strongly magnetic WDs as well.

1. The methylidinium cation CH^+

In Ref. 58, the CH^+ cation has been studied at the CCSD and CCSDT levels of theory for an increasing magnetic-field strength and various orientations. In that study, the CCSDT results were practically indistinguishable from the exact full configuration interaction (FCI) predictions. Here, the approximate ff-CC2 and ff-CC3 methods are tested for the same system. The accuracy of CC3 predictions is examined in comparison to the CCSDT level of theory, while the performance of the CC2 approximation is tested against CCSD.

Calculations were carried out at the ground state field-free CCSD/cc-pVDZ equilibrium distance of $2.1275\,a_0$ and are plotted in Fig. 3 against the magnetic-field strength. The $^1\Sigma^+$ ground state (purple) with $1\sigma^2 2\sigma^2 3\sigma^2$ electronic configuration was chosen as reference for subsequent EOM-CC calculations. The excited states that were targeted are the $^1\Pi$ state (red and blue) and the $^1\Delta$ state (yellow). Both are doubly degenerate states described by a $1\sigma^2 2\sigma^2 3\sigma^1 1\pi^1$ and a $1\sigma^2 2\sigma^2 1\pi^2$ configuration, respectively. The energetically higher-lying $^1\Delta$ state has a predominant double-excitation character with respect to the reference. As such, it is not well described at the CCSD level, as already noted in Ref. 58. For an in-depth discussion on the behavior of the methylidinium cation in the presence of magnetic field, see Refs. 58 and 65.

In general, CC2 is not able to describe states with predominant double-excitation character. For this reason, CC2 results for the $^1\Delta$ state (yellow) are absent in the calculations. Regarding states with predominant single-excitation character, CC2 energies exhibit a positive shift that reaches up to $3.6 \cdot 10^{-2} E_h$ relative to CCSDT throughout the calculations. If the excitation does not acquire a double-excitation character, a rather reasonable description is obtained. The shift is more or less constant and does not influence the excitation energies nor the overall behavior much.

In the upper left panel of Fig. 3, the results for the parallel magnetic-field orientation are presented. Here, the reference and the predominantly singly excited states are well behaved. For these states, the deviation of CC2 results from CCSDT ($\sim 10^{-2}\ E_h$) is about one order of magnitude larger than the CCSD results ($\sim 10^{-3}\ E_h$). Energies at the CC3 level, however, have a mean deviation at the order of $\sim 10^{-4}\ E_h$. For the $^1\Delta$ state, which is a state with a predominant double-excitation character, the mean error at the CC3 level drops from $3.6 \cdot 10^{-2} E_h$ for CCSD by more than half to $1.2 \cdot 10^{-2} E_h$.

As noted in Ref. 58, the avoided crossings that arise between the original $^1\Delta$ state and the other states in all nonparallel magnetic-field orientations result in a transfer of the double-excitation character. This is problematic because a single state is not described with the same accuracy for every magnetic-field strength. In addition, the field strength at which the avoided crossing is encountered is strongly method dependent. Such a transfer is most clearly seen at an orientation of 30°, where between 0.1 and $0.6 B_0$, two avoided crossings occur between the $4^1A(^1\Delta)$ state (yellow) and the $3^1A(^1\Pi)$ state (blue). Notably, CC2 proves to be particularly inappropriate for these cases as the curve for the state arising from $^1\Pi$ (blue) is qualitatively very different compared to the predictions at more accurate levels of theory. The reason for the poor description of this state at the CC2 level stems from the fact that the predominant double-excitation character cannot be described within CC2 and the avoided crossing is simply not found. Instead, the curve follows the higher-lying 4^1A state for field strengths greater than $0.1 B_0$. Hence, for CC2, the resulting artificial state (blue dotted curve) is a nonphysical combination of two different (physical) states. For CC2, this is a general problem for any avoided crossing involving states with single- and double-excitation character.

CC3 results on the other hand give a consistent description of states in the non-parallel magnetic-field orientations and offer a significant improvement relative to the CCSD results. The results obtained around the avoided crossing at CC3 are much closer to CCSDT predictions as compared to CCSD. Additionally, the deviation of CC3 results relative to CCSDT is about half of the deviation of CCSD relative to CCSDT when a predominant double-excitation character is present. Specifically for the more complicated 3^1A and 4^1A cases (blue and yellow, respectively), the mean deviation drops by one order of magnitude to $10^{-3} E_h$ at CC3 compared to CCSD. This observation is consistent with the results for the $^1\Delta$ state in the parallel orientation. In the case of a predominant single-excitation character, the mean deviation at the CC3 level relative to the CCSDT results is $5.7 \cdot 10^{-4} E_h$ with a maximum error of $1.6 \cdot 10^{-3} E_h$. Compared to CCSD, the mean deviation is one order of magnitude smaller and the maximum error is less than half. In fact, the CC3 results are practically indistinguishable from CCSDT when a single-excitation character is dominant.

The study of the CH^+ cation shows a problematic behavior of the CC2 method for systems where avoided crossings with states of relevant double-excitation character appear. In such cases, CC2 can yield nonphysical results. Using CC3 as an approximate triples cor-

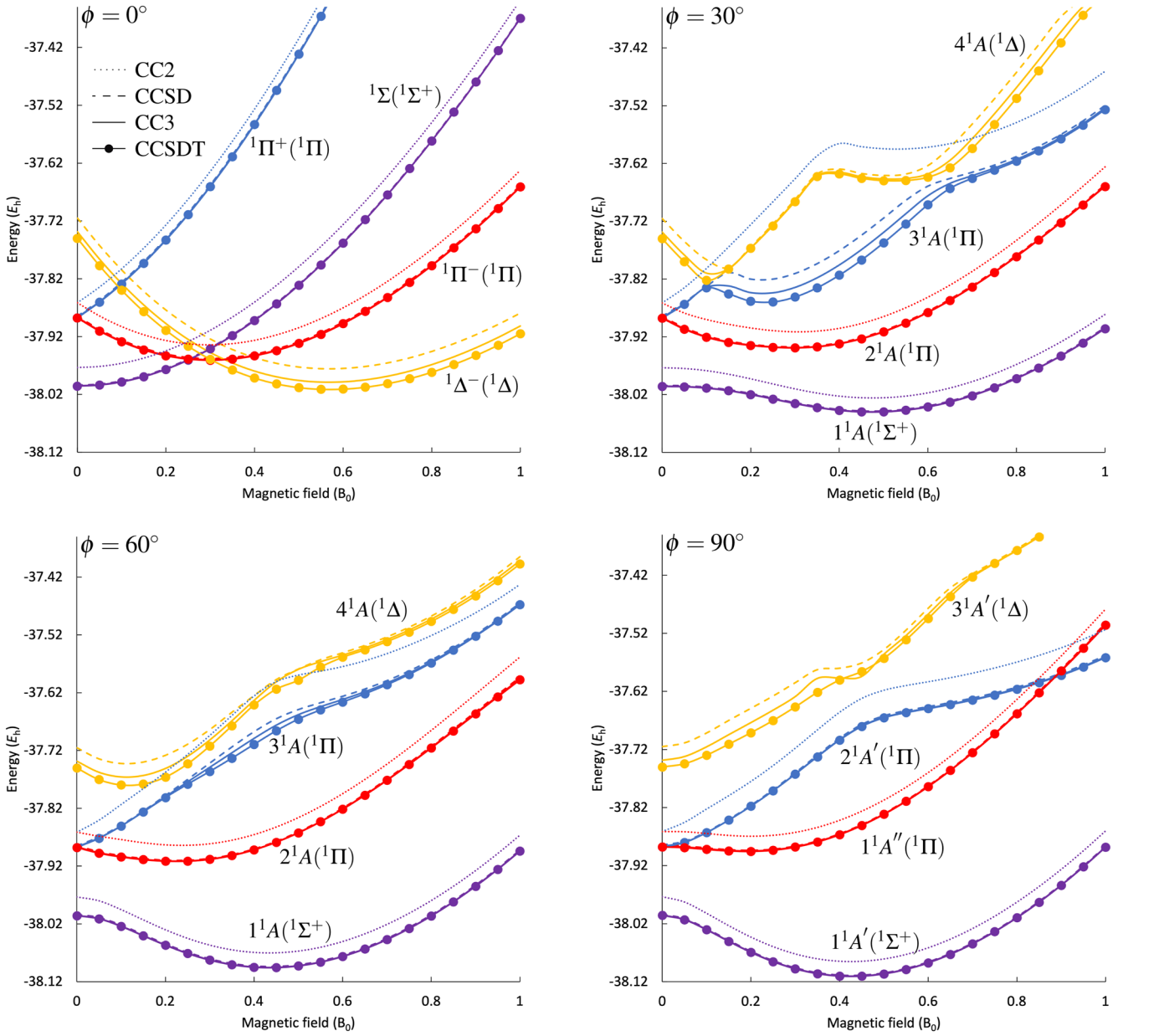

FIG. 3. The low-lying singlet states of CH^+ as a function of the magnetic-field strengths for different orientations of the molecule at the (EOM-)CC2, CCSD, CC3, and CCSDT levels of theory with the cc-pVDZ basis set.

rection works rather well, even in cases where the state acquires a significant double-excitation character.

2. The CH radical

The CH radical was studied at the (EOM-)CC2, CCSD, CC3, and CCSDT levels of theory using an unc-cc-pVDZ basis set at a field-free optimized bond length at the CCSD level of 2.1431 bohrs. In Figs. 4 and 5, a comparison of the CC2 and CC3 results with CCSDT for the skewed ($\phi = 60°$) and perpendicular ($\phi = 90°$) orientations, respectively, is presented. In these plots, the energy of low-lying singlet states of the molecule is plotted as a function of the magnetic-field strength. Respective calculations for the parallel and $\phi = 30°$ orientations of the magnetic field relative to the molecular bond and results at the CCSD level can be found in Ref. 65.

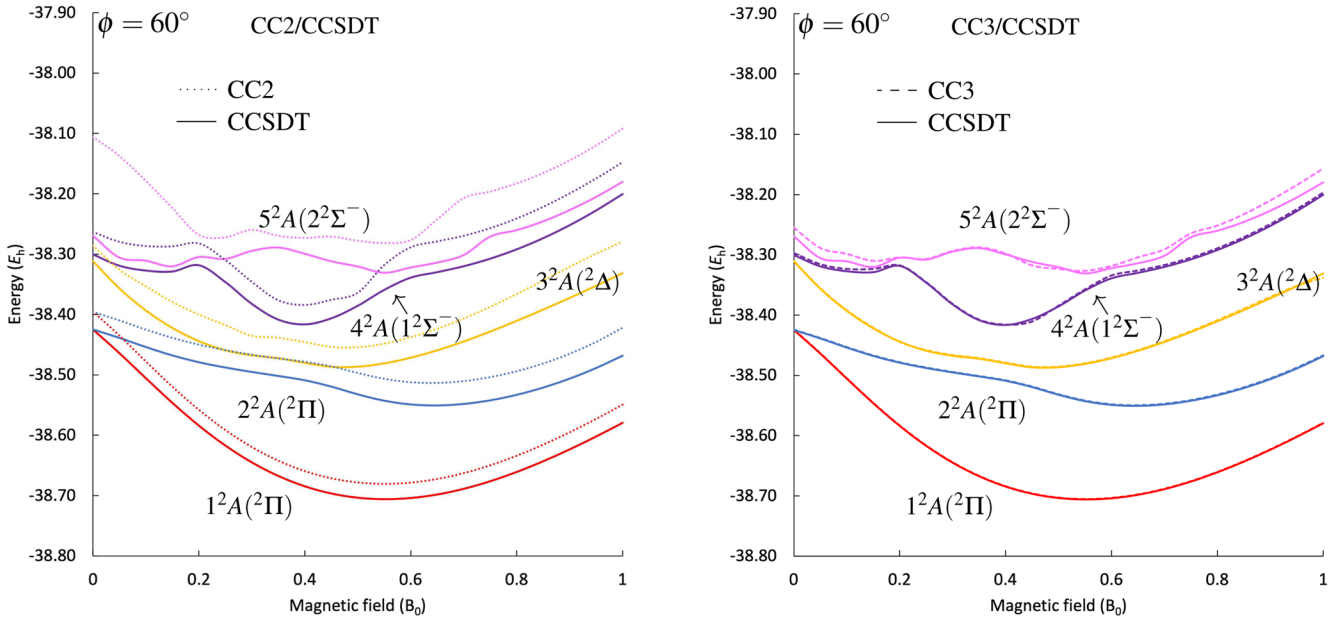

FIG. 4. Comparison of CC2 (left panel) and CC3 (right panel) with CCSDT results obtained using the unc-cc-pVDZ basis set for four low-lying doublet states of the CH radical. The magnetic field is oriented at a 60° angle with respect to the molecular bond.

Since the CH radical is an open-shell system with a doubly degenerate $^2\Pi$ ground state with a predominant $1\sigma^2 2\sigma^2 3\sigma^2 1\pi^1$ electronic configuration, it constitutes a challenging test-case for the ff-EOM-CC treatment: Choosing one of the components of the $^2\Pi$ state as the reference state introduces an artificial break in their degeneracy, as only one of the two Π components is treated as an excited EOM-CC state. The severity of this effect is quantified by the energy difference. It amounts to about $\sim 10^{-4}$ E_h at the CC2 and CCSD levels of theory, about $\sim 10^{-5}$ E_h for CC3, and about $\sim 10^{-6}$ E_h for CCSDT, showing that, as expected, the problem diminishes when improving the correlation treatment towards FCI. The degenerate excited $^2\Delta$ state described by a $1\sigma^2 2\sigma^2 3\sigma^1 1\pi^2$ configuration was studied as well. For this state, one of the components (yellow) is characterized predominantly by a single excitation relative to the reference, while the other component is doubly excited and not targeted here. Furthermore, two excited $^2\Sigma^-$ states were studied. The energetically lower-lying one, $1^2\Sigma^-$, has a predominant $3\sigma^{\uparrow} 1\pi^{-\downarrow} 1\pi^{+\downarrow}$ configuration (purple), while the second state $2^2\Sigma^-$ (pink) has a multideterminantal character with predominant $\left(3\sigma^{\downarrow} 1\pi^{-\downarrow} 1\pi^{+\uparrow} + 3\sigma^{\downarrow} 1\pi^{-\uparrow} 1\pi^{+\downarrow}\right)$ configuration. Similar to the case of the $^2\Delta$ state, one of the determinants is doubly excited with respect to the reference. Description of the $2^2\Sigma^-$ state is particularly challenging. In principle, EOM approaches are applicable to excited states with a multiconfigurational character. However, for such a description to work well, the strongly contributing determinants need to be singly excited with respect to the reference,[86] which is not the case here. Additionally, due to symmetry breaking in the CC reference state, the configurations no longer have the same weight.

Overall, it is noted that the performance of ff-CC2 is able to provide a qualitative description for states with single-excitation character. It has large errors for excited states with mixed excitation character and completely fails to target the doubly excited $^2\Delta$ component. Ff-CC3 on the other hand yields energies very close to CCSDT. Further discussion in the following paragraphs on the performance of CC2 and CC3 is focused on the skewed 60° and perpendicular 90° magnetic-field orientations relative to the molecular bond.

In Fig. 4 (skewed 60° orientation), the CC2 and CC3 energies can be compared to the CCSDT reference. Results at the CC3 level exhibit deviations from CCSDT at the order of about 10^{-4} E_h in the case of a predominant single-excitation character. These deviations are smaller by one order of magnitude as compared to CCSD. In the case of significant double-excitation character, the deviation from CCSDT is at the order of 10^{-2} E_h. Compared to CCSD, the error is reduced by a factor of two. The CC2 method on the other hand still offers a crude qualitative description of the three lowest-energy states but proves particularly problematic if not unphysical for the states arising from the $^2\Sigma^-$ states (purple and pink). The progression of the 4^2A (purple) and 5^2A (pink) states at the CC2 level with increasing magnetic-field strength is in many cases qualitatively very different compared to the CCSDT reference and the more accurate methods and apparently wrong. For example, the response of the 5^2A state (pink) to an increasing magnetic field at the CCSDT level is described as follows: The energy is relatively constant for field strengths between $B = 0$–$0.2B_0$. It rises for stronger fields until ~ 0.35 B_0, reaching a local maximum due to an avoided crossing with a higher-lying state. The state is then slightly stabilized up to $B = 0.6B_0$ after which the diamagnetic response becomes dominant. In

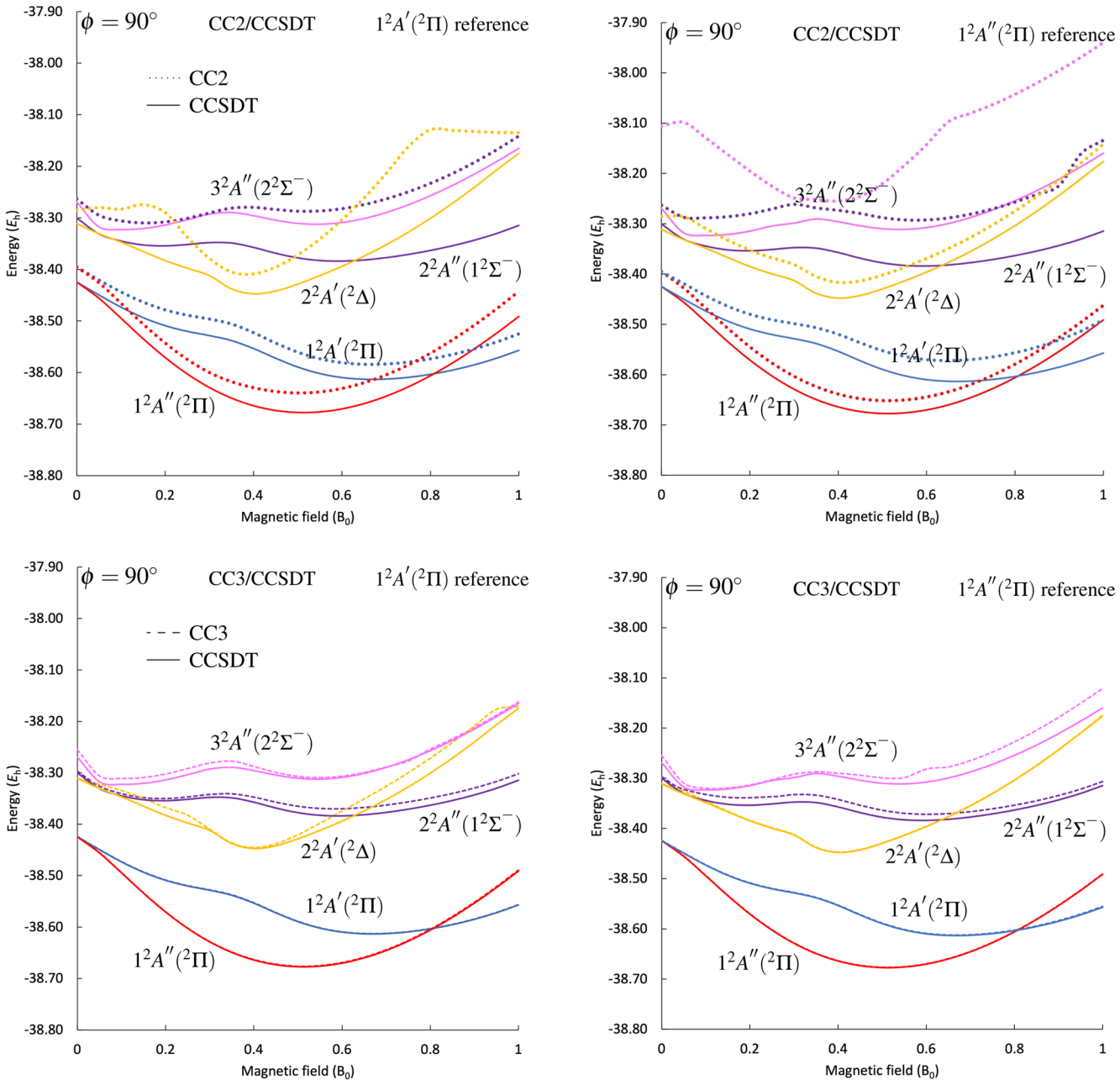

FIG. 5. Comparison of CC2 (upper panel) and CC3 (lower panel) with CCSDT results obtained using the unc-cc-pVDZ basis set for the low-lying states of the CH radical with different reference states: $1^2A'$ (blue) left column, $1^2A''$ (red) right column. The magnetic-field orientation is perpendicular to the molecular bond.

addition, the state is energetically close to the 4^2A state (purple). At the CC2 level, however, the 5^2A state (pink) starts off energetically higher in the field-free case with a very large error of $0.16E_h$ relative to CCSDT. As seen in the left panel of Fig. 4, the development of the state is qualitatively different up to $B = 0.2B_0$: The state is gradually stabilized and approaches the CCSDT reference. For $B \geq 0.2B_0$, the CC2 deviation relative to CCSDT is lower by one order of magnitude ($\sim 10^{-2}$ E_h) compared to the field-free case. Nonetheless, the energy development of this state exhibits features that are absent from the results from more accurate methods, like two avoided crossings with the 4^2A (purple) state at $B = 0.2B_0$ and $B = 0.6B_0$. All these qualitative differences constitute a strong indication that the character of

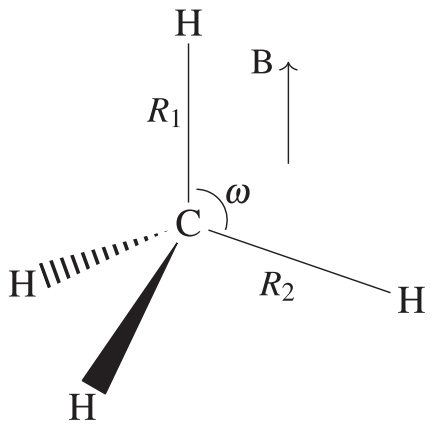

FIG. 6. Methane with the magnetic field oriented parallel to one of the C–H bonds. C_3 symmetry.

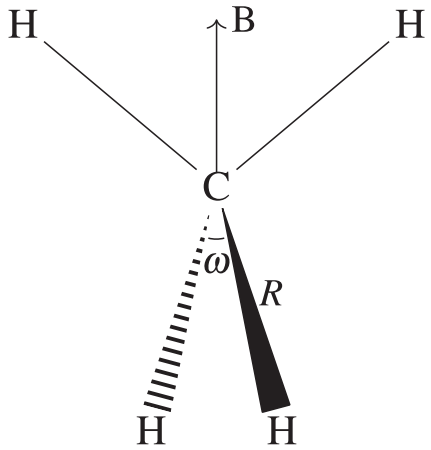

FIG. 7. Methane with the magnetic field oriented parallel to the bisector of a H–C–H angle. S_4 symmetry.

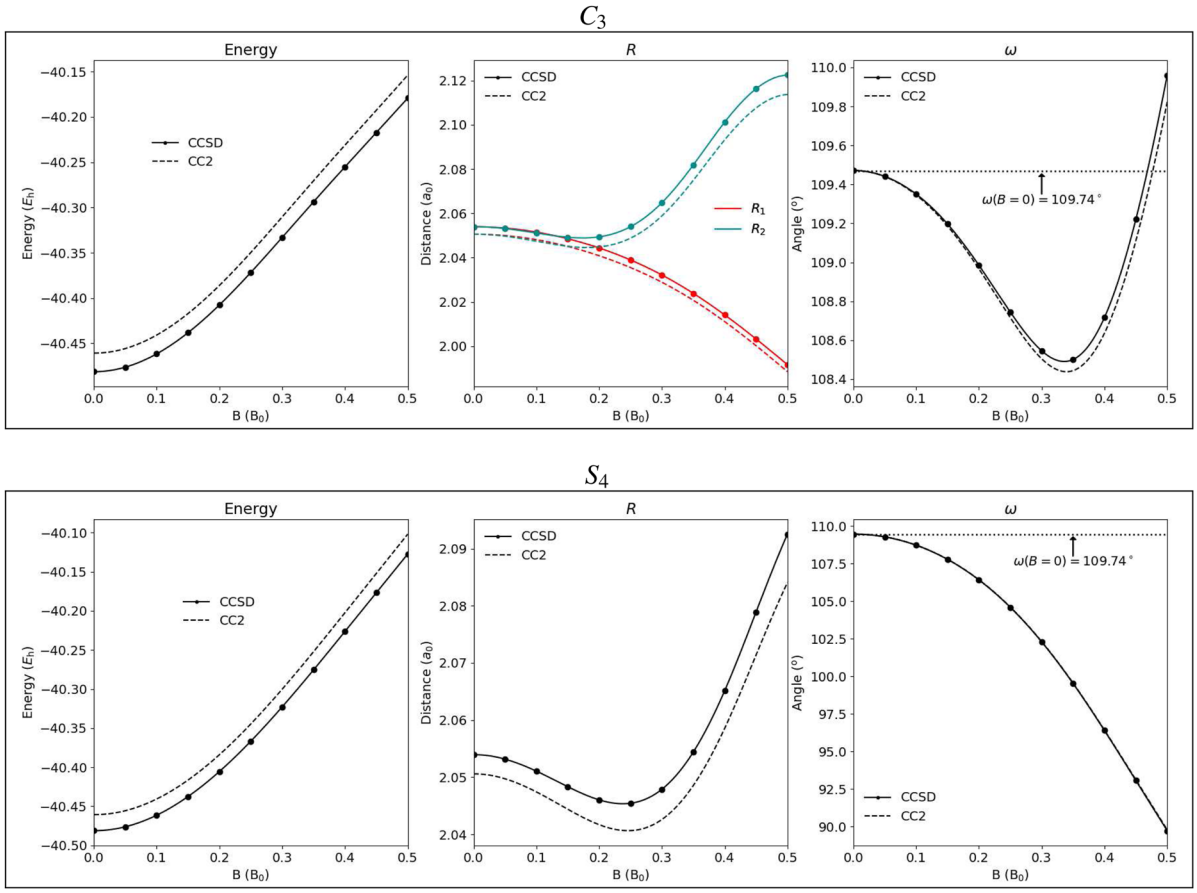

FIG. 8. Energies in E_h (left), as well as bond lengths in a_0 (middle) and angles in degrees (right) for the energetically lowest singlet state of the methane molecule at the optimized geometry at the CCSD (full line) and CC2 (dashed line) levels of theory as a function of the magnetic-field strength for two different orientations of the magnetic field with respect to the molecule: upper panel B parallel to a C–H bond (C_3 symmetry), lower panel B parallel to the bisector of the H–C–H angle (S_4 symmetry).

the state at the CC2 level is at least over a range of field strengths qualitatively different compared to CCSDT and that the CC2 results are hence unphysical. The CC3 curve for this state on the other hand clearly follows the CCSDT reference over the complete range of field strengths. It can be noted that the deviations are small in the range between 0.2 and $0.6B_0$, where a single-excitation character dominates.

The results for the magnetic-field orientation perpendicular to the bond are shown in Fig. 5. Here, we compare two independent series of CC2 and CC3 calculations using different CC reference states, i.e., the two components of the field-free ground state $^2\Pi \rightarrow {}^2A', {}^2A''$ (blue and red, respectively) in order to judge the quality of prediction. Again, the results are compared to CCSDT reference calculations. It is expected that the choice of reference should become less important for the EOM-CC states when approaching the FCI limit. This is indeed what is observed for the CCSDT results. They differ only slightly for the different choice of reference. In contrast, the CC2 method performs poorly for this test. First, it fails to consistently target all the states studied. For example, it was not possible to target the $3^2A''$ (pink) state using the A' (blue) reference. Second, the results are in many cases qualitatively different when using different reference states. Moreover, the magnetic-field strength at which the two components of the field-free ground state, i.e., the $1^2A'$ (blue) and $1^2A''$ (red) states, cross is not predicted consistently at the CC2 level. The states cross at about $0.75B_0 \approx 180$ kT when using $1^2A'$ (blue) as reference and at about $0.9B_0 \approx 210$ kT when the $1^2A''$ (red) is used. This amounts to a huge difference of about 30 kT. The CC3 approach on the other hand produces results very close to those at the CCSDT level. The two states arising from the $^2\Pi$ state are practically indistinguishable at the CC3 and CCSDT levels of theory. The difference at their crossing point when using the two references is about $0.05B_0 = 1$ kT at CC3 and smaller then <0.01 $B_0 \approx 0.2$ kT at CCSDT. The three higher-energy states are qualitatively in agreement between the two methods with larger deviations when a double-excitation character is present. On closer inspection, the $3^2A''$ state (pink) is described slightly better with the $1^2A'$ (blue) reference, while the $2^2A'$ state (yellow) is described better with the $1^2A''$ (red) reference. This behavior is due to contributions from doubly excited determinants, which differ depending on the reference CC state.

An analogous comparison for the parallel and $\phi = 30°$ orientation of the magnetic field is presented in Ref. 65. For the 30° orientation, the observations are very similar to those at 60°. For the parallel case, the performance of CC*n* approximations is more consistent among the different orientations as, due to symmetry, the mixing between states is much more limited.

The calculations presented here consistently show that CC3 offers a satisfactory approximation to CCSDT even when a complex multiconfigurational character that arises from both single and double excitations is present. CC2 offers a crude qualitative description for the first few excited states that have a strong single-excitation character. Even for those cases, however, quantitative results, like the crossing point between states, are inconsistent and depend on which state has been chosen as the CC reference. For the states with a more complex multiconfigurational character, CC2 results are found to be unreliable.

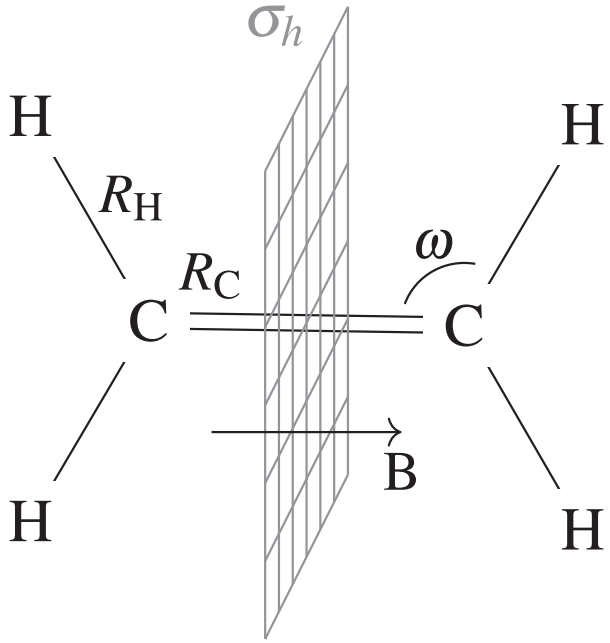

FIG. 9. Ethylene in a magnetic field oriented parallel to the C=C bond. C_{2h} symmetry. The mirror plane σ_h perpendicular to the magnetic field is depicted by the gray grid.

C. Geometry optimizations in a strong magnetic field

Geometry optimizations were performed on methane (CH_4) and ethylene (C_2H_4) in the presence of a magnetic field for different magnetic-field orientations and strengths. The unc-cc-pVTZ basis set was used to perform calculations at the ff-CCSD and ff-CC2 levels of theory. A geometry optimization based on numerical gradients was carried out for magnetic-field strengths up to $0.5B_0$ using a $0.05B_0$ step. The optimizer module of CFOUR[48,108] was

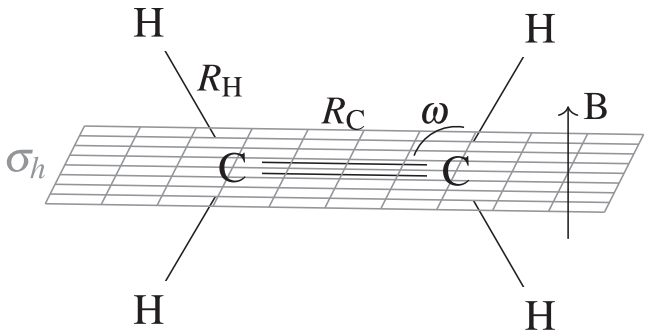

FIG. 10. Ethylene in a magnetic field parallel to the molecular plane and oriented perpendicular to the C=C bond. C_{2h} symmetry. The mirror plane σ_h perpendicular to the magnetic field is depicted by the gray grid.

used, while the post-HF results were obtained using the QCUMBRE program[47] in conjunction with an interface to CFOUR for the underlying ff-HF-SCF solution.

1. Methane CH_4

In the field-free case, the symmetry of methane is described by the tetrahedral T_d point group. Two orientations of the molecule relative to the magnetic field were studied. In the first one, one of the C–H bonds coincides with the magnetic field, reducing the symmetry to C_3 as depicted in Fig. 6. In the second orientation, depicted in Fig. 7, the bisector of one of the H–C–H angles defines the magnetic-field orientation, which reduces the symmetry to S_4. In both cases, geometry optimizations were performed for the energetically lowest-lying singlet state $^1A(^1A_1)$.

The results for geometry optimization, i.e., the energy at the constrained optimized geometry as well as the geometric parameters as a function of the magnetic-field strength, are plotted in Fig. 8. Regarding the C_3 case, the CC2 results for geometry parameters reproduce the CCSD behavior extremely well. At the CC2 level, bond lengths are about $0.004\,a_0$ shorter compared to CCSD predictions. The angles deviate by only 0.1°. In the S_4 case, similar trends are observed. The CC2 bond lengths are shorter by only ~0.004 a_0 at CC2 compared to CCSD and angles deviate at most by 0.06°. The predictions for geometrical parameters at the CC2 level are thus nearly identical to those at CCSD. The energetic difference between CCSD and CC2 results of around $22\,mE_h$ is also rather constant for different magnetic-field strengths for the two orientations.

The response of molecular geometry to the increasing magnetic field together with a study of the excited states can be found in Ref. 65. Beyond these findings, methane has also been previously studied in Ref. 119 concerning its stability and the formation of exotic structures in the presence of a magnetic field at the ff-TDDFT level. In magnetic fields stronger than $0.5B_0$, a peculiar "fan-like" geometry of CH_4 was predicted, resulting from a paramagnetic-bond formation in magnetic fields stronger than $0.5B_0$.[119]

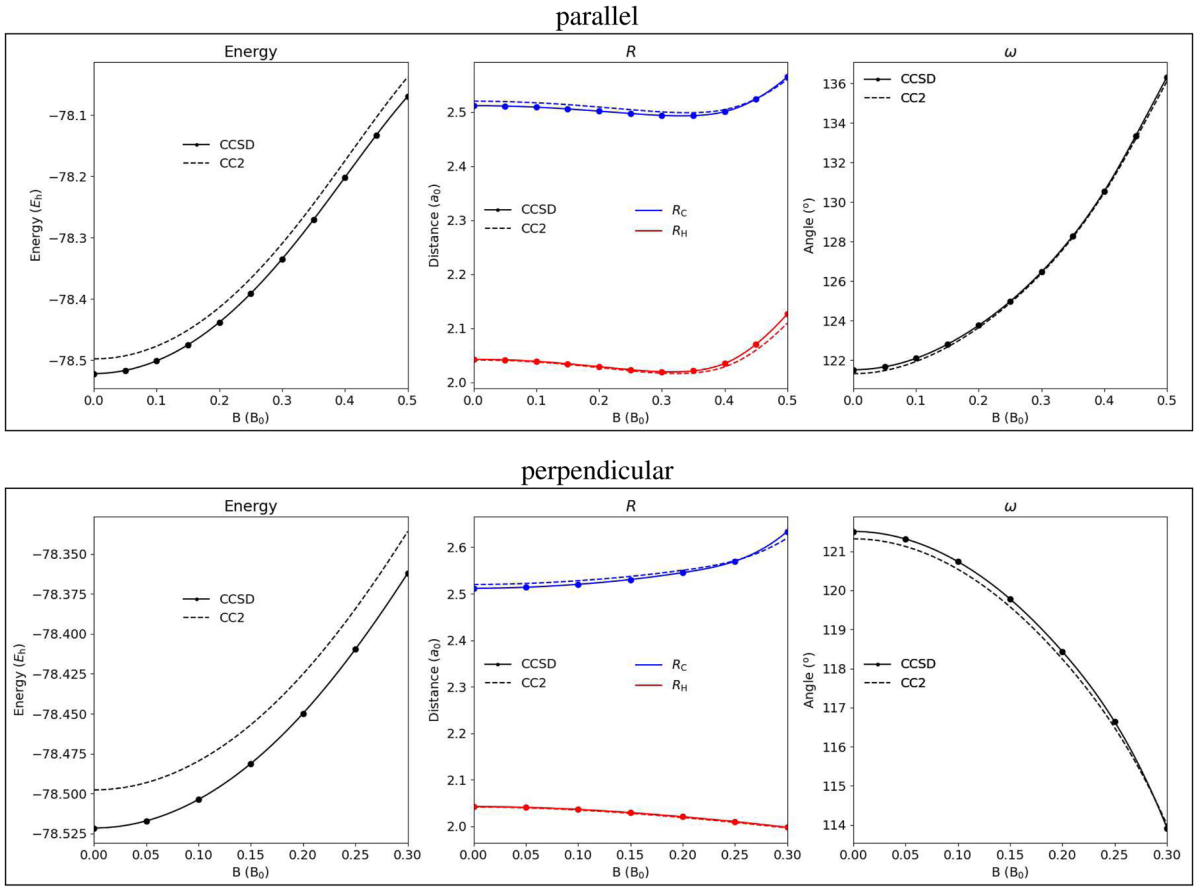

FIG. 11. Energies in E_h (left), as well as bond lengths in a_0 (middle) and angles in degrees (right) for the energetically lowest singlet state of the ethylene molecule at the optimized geometry at the CCSD (full line) and CC2 (dashed line) levels of theory as a function of the magnetic-field strength for two different orientations of the magnetic field with respect to the molecule: upper panel *B* parallel to the C=C bond, lower panel *B* in-plane perpendicular to the C=C bond.

2. Ethylene CH_2=CH_2

Two magnetic-field orientations were studied in the case of ethylene, which are depicted in Figs. 9 and 10. In both cases, the symmetry is reduced from D_{2h} in the absence of a magnetic field to two distinct C_{2h} subgroups. In the first case, the magnetic field is oriented parallel to the C=C bond and in the second case it is perpendicular to the C=C bond and lies within the molecular plane. The gray grid in the figures depicts the different mirror planes. In spite of symmetry reduction, the hydrogen and carbon nuclear centers remain symmetry equivalent. In regard to constrained geometry optimization for the energetically lowest-lying singlet state ${}^1A_g({}^1A_g)$, the degrees of freedom are the C=C and C–H bond lengths, R_C and R_H, respectively, together with the C–C–H angle ω.

The energy at the optimized geometry and the geometric parameters of the molecule are plotted for the two different orientations as a function of magnetic field in Fig. 11. The CC2 and CCSD predictions are in qualitative agreement with each other. As expected, the CC2 total energies are higher than the CCSD energies for different magnetic-field strengths and orientations by a nearly constant shift of $0.025E_h$. Similar to the methane study, the geometric parameters only show minimal deviation between the two approaches, with a mean deviation of 0.006 bohrs for the bond lengths and 0.1° for the angle. It is worth noting that the molecule dissociates for field strengths greater than 0.30 B_0 in the perpendicular orientation of the magnetic field. This prediction is consistent at both the CC2 and CCSD levels of theory.

A detailed discussion of the response of geometry to the magnetic field together with an investigation of the spectrum in the presence of a magnetic field for ethylene can be found in Ref. 65.

The calculations for methane and ethylene show that the CC2 method performs very well against CCSD for geometry optimizations. The geometrical parameters obtained at the CC2 level are practically indistinguishable from the CCSD results.

V. CONCLUSION

In this paper, the CC2 and CC3 methods, as well as the respective EOM-CC approach have been implemented for calculations of ground and excited states of molecules in finite magnetic fields. These methods approximate the standard CC truncations, i.e., CCSD and CCSDT, respectively, and lower the scaling by one order of magnitude relative to their parent methods.

Various systems were studied in the presence of a magnetic field using these approximate CC*n* methods and were compared to calculations using the standard CC truncations to test their performance. The triplet states of the Mg atom were studied at the CCSD, CC3, and CCSDT levels of theory. B-λ curves were generated using an adaptation of a previously reported extrapolation scheme.[58] These calculations have been essential for the assignment of a spectrum from a strongly magnetic white dwarf star.[118] The CC3 approach enabled calculations with larger basis sets that give an accuracy similar to that of CCSDT. Additionally, the diatomic cation CH^+ and radical CH, which are candidate molecules to occur in the atmosphere of strongly magnetic white dwarfs, were studied at the (EOM-)CC2, (EOM-)CCSD, (EOM-)CC3, and (EOM-)CCSDT levels of theory at various magnetic-field strengths and orientations. The CC2 approach was found to yield nonphysical results when avoided crossings between excited states with a predominant double-excitation character are involved. CC3 on the other hand is shown to replicate the CCSDT behavior for ground and excited states with a predominant single-excitation character. It even manages to capture a large extent of the double-excitation character. Geometry optimizations were performed for the energetically lowest-lying singlet state of the small organic molecules CH_4 and C_2H_4 in different highly symmetric magnetic-field orientations and different field strengths at the CC2 and CCSD levels of theory. The study of these systems contributes to a better understanding of the geometric response of small molecules to the magnetic field. Optimized geometry parameters at the CC2 level of theory practically replicate the CCSD results.

The results in this paper show that CC2 may be a good alternative to CCSD for larger systems, particularly for geometry optimizations. On the other hand, EOM-CC2 suffers from the inability to account for excited states with a double-excitation character. This can lead to unphysical results, when avoided crossings with such states are involved. The latter, however, is more the rule than exception for species in strong magnetic fields, particularly, but not only, in skewed orientations of the field. For this reason, the EOM-CC2 approach should be applied only if avoided crossings of this kind can be excluded.

The CC3 method has been demonstrated to have merits in finite magnetic-field calculations. For both ground and excited states with predominant single-excitation character, results obtained at the (EOM-)CC3 level of theory are essentially indistinguishable from the (EOM-)CCSDT results. In addition, EOM-CC3 offers a significant improvement relative to EOM-CCSD for excited states with predominant double-excitation character with results closer qualitatively to those of full EOM-CCSDT. The more favorable scaling of N^7 as compared to N^8 of CCSDT allows an approximate treatment of triple corrections and high-accuracy predictions for larger systems with larger basis sets.

SUPPLEMENTARY MATERIAL

The raw arithmetic data used for the generation of the plots is collected in the supplementary material. These include the energies of triplet states of Mg as a function of the magnetic-field strength and the generated B-λ curves, the total energies of the states of CH^+ and CH as a function of the magnetic-field strength for different magnetic-field orientations, and the results of geometry optimizations for methane and ethylene in different magnetic-field strengths.

ACKNOWLEDGMENTS

The authors thank Professor Dr. Jürgen Gauss for valuable discussions. This work has been supported by the Deutsche Forschungsgmeinschaft under Grant No. STO 1239/1-1.

AUTHOR DECLARATIONS

Conflict of Interest

The authors have no conflicts to disclose.

Author Contributions

Marios-Petros Kitsaras: Conceptualization (supporting); Formal analysis (equal); Investigation (equal); Methodology (equal); Software (lead); Validation (equal); Writing – original draft (equal); Writing – review & editing (equal). **Laura Grazioli**: Formal analysis (supporting); Investigation (supporting); Validation (supporting); Writing – review & editing (supporting). **Stella Stopkowicz**: Conceptualization (lead); Formal analysis (equal); Funding acquisition (lead); Investigation (equal); Methodology (equal); Supervision (lead); Validation (equal); Writing – original draft (equal); Writing – review & editing (equal).

DATA AVAILABILITY

The data that support the findings of this study are available within the article and its supplementary material.

REFERENCES

[1] P. Schmelcher, L. S. Cederbaum, P. Schmelcher, and L. S. Cederbaum, "Molecules in strong magnetic fields: Some perspectives and general aspects," Int. J. Quantum Chem. **64**, 501–511 (1997).

[2] *Chemistry at Extreme Conditions*, edited by M. R. Manaa (Elsevier, 2005).

[3] A. Fridman, *Plasma Chemistry* (Cambridge University Press, Cambridge, 2008).

[4] E. I. Tellgren, T. Helgaker, and A. Soncini, "Non-perturbative magnetic phenomena in closed-shell paramagnetic molecules," Phys. Chem. Chem. Phys. **11**, 5489 (2009).

[5] K. Motzfeldt, *High Temperature Experiments in Chemistry and Materials Science* (John Wiley & Sons, Ltd., Chichester, UK, 2012).

[6] P. Schmelcher, "Molecule formation in ultrahigh magnetic fields," Science **337**, 302–303 (2012).

[7] K. K. Lange, E. I. Tellgren, M. R. Hoffmann, and T. Helgaker, "A paramagnetic bonding mechanism for diatomics in strong magnetic fields," Science **337**, 327–331 (2012).

[8] M. Miao, Y. Sun, E. Zurek, and H. Lin, "Chemistry under high pressure," Nat. Rev. Chem. **4**, 508–527 (2020).

[9] J. L. Margrave, "High-temperature chemistry," in *AccessScience* (McGraw Hill, 2020).

[10] W. Rosner, G. Wunner, H. Herold, and H. Ruder, "Hydrogen atoms in arbitrary magnetic fields. I. Energy levels and wavefunctions," J. Phys. B: At. Mol. Phys. **17**, 29–52 (1984).

[11] P. Schmelcher, L. S. Cederbaum, and H. D. Meyer, "Electronic and nuclear motion and their couplings in the presence of a magnetic field," Phys. Rev. A **38**, 6066–6079 (1988).

[12] P. Schmelcher, L. S. Cederbaum, and H. D. Meyer, "On the validity of the Born-Oppenheimer approximation in magnetic fields," J. Phys. B: At., Mol. Opt. Phys. **21**, L445–L450 (1988).

[13] P. Schmelcher and L. S. Cederbaum, "Molecules in strong magnetic fields: Properties of atomic orbitals," Phys. Rev. A **37**, 672–681 (1988).

[14] P. Schmelcher and L. S. Cederbaum, "On molecules and ions in strong magnetic fields," Int. J. Quantum Chem. **40**, 371–385 (1991).

[15] S. Jordan, P. Schmelcher, W. Becken, and W. Schweizer, "Evidence for helium in the magnetic white dwarf GD 229," Astron. Astrophys. **336**, L33–L36 (1998).

[16] A. Soncini and P. Fowler, "Non-linear ring currents: Effect of strong magnetic fields on π-electron circulation," Chem. Phys. Lett. **400**, 213–220 (2004).

[17] E. I. Tellgren, A. Soncini, and T. Helgaker, "Nonperturbative *ab initio* calculations in strong magnetic fields using London orbitals," J. Chem. Phys. **129**, 154114 (2008).

[18] E. I. Tellgren, A. M. Teale, J. W. Furness, K. K. Lange, U. Ekström, and T. Helgaker, "Non-perturbative calculation of molecular magnetic properties within current-density functional theory," J. Chem. Phys. **140**, 034101 (2014).

[19] S. Sen, K. K. Lange, and E. I. Tellgren, "Excited states of molecules in strong uniform and nonuniform magnetic fields," J. Chem. Theory Comput. **15**, 3974–3990 (2019).

[20] S. Sun, D. Williams-Young, and X. Li, "An *ab initio* linear response method for computing magnetic circular dichroism spectra with nonperturbative treatment of magnetic field," J. Chem. Theory Comput. **15**, 3162–3169 (2019).

[21] S. Stopkowicz, J. Gauss, K. K. Lange, E. I. Tellgren, and T. Helgaker, "Coupled-cluster theory for atoms and molecules in strong magnetic fields," J. Chem. Phys. **143**, 074110 (2015).

[22] F. Hampe and S. Stopkowicz, "Equation-of-motion coupled-cluster methods for atoms and molecules in strong magnetic fields," J. Chem. Phys. **146**, 154105 (2017).

[23] J. W. Furness, J. Verbeke, E. I. Tellgren, S. Stopkowicz, U. Ekström, T. Helgaker, and A. M. Teale, "Current density functional theory using meta-generalized gradient exchange-correlation functionals," J. Chem. Theory Comput. **11**, 4169–4181 (2015).

[24] S. Reimann, A. Borgoo, J. Austad, E. I. Tellgren, A. M. Teale, T. Helgaker, and S. Stopkowicz, "Kohn–Sham energy decomposition for molecules in a magnetic field," Mol. Phys. **117**, 97–109 (2019).

[25] S. Lehtola, M. Dimitrova, and D. Sundholm, "Fully numerical electronic structure calculations on diatomic molecules in weak to strong magnetic fields," Mol. Phys. **118**, e1597989 (2020); arXiv:1812.06274.

[26] A. Pausch and W. Klopper, "Efficient evaluation of three-centre two-electron integrals over London orbitals," Mol. Phys. **118**, e1736675 (2020).

[27] C. Holzer, A. Pausch, and W. Klopper, "The GW/BSE method in magnetic fields," Front. Chem. **9**, 746162 (2021).

[28] S. Blaschke and S. Stopkowicz, "Cholesky decomposition of complex two-electron integrals over GIAOs: Efficient MP2 computations for large molecules in strong magnetic fields," J. Chem. Phys. **156**, 044115 (2022); arXiv:2108.11370.

[29] L. Monzel, A. Pausch, L. D. M. Peters, E. I. Tellgren, T. Helgaker, and W. Klopper, "Molecular dynamics of linear molecules in strong magnetic fields," J. Chem. Phys. **157**, 054106 (2022).

[30] R. H. Garstang, "Atoms in high magnetic fields (white dwarfs)," Rep. Prog. Phys. **40**, 105–154 (1977).

[31] S. Jordan, "Magnetic fields in White Dwarfs and their direct progenitors," Proc. Int. Astron. Union **4**, 369–378 (2008).

[32] L. Ferrario, D. de Martino, and B. T. Gänsicke, "Magnetic white dwarfs," Space Sci. Rev. **191**, 111–169 (2015).

[33] D. T. Wickramasinghe and L. Ferrario, "Magnetism in isolated and binary white dwarfs," Publ. Astron. Soc. Pac. **112**, 873–924 (2000).

[34] E. L. Degl'Innocenti and M. Landolfi, *Polarization in Spectral Lines* (Springer Netherlands, Dordrecht, 2004).

[35] R. J. W. Henry and R. F. Oconnell, "On the magnetic field in the white dwarf GRW + 70.8247 deg," Astrophys. J. **282**, L97 (1984).

[36] R. J. W. Henry and R. F. Oconnell, "Hydrogen spectrum in magnetic white dwarfs: H-alpha, H-beta and H-gamma transitions," Publ. Astron. Soc. Pac. **97**, 333 (1985).

[37] H. Forster, W. Strupat, W. Rosner, G. Wunner, H. Ruder, and H. Herold, "Hydrogen atoms in arbitrary magnetic fields. II. Bound-bound transitions," J. Phys. B: At. Mol. Phys. **17**, 1301–1319 (1984).

[38] J. L. Greenstein, "The identification of hydrogen in GRW +70 deg 8247," Astrophys. J. **281**, L47 (1984).

[39] J. L. Greenstein, R. J. W. Henry, and R. F. Oconnell, "Futher identifications of hydrogen in GRW +708247," Astrophys. J. **289**, L25 (1985).

[40] G. D. Schmidt, R. G. Allen, P. S. Smith, and J. Liebert, "Combined ultraviolet-optical spectropolarimetry of the magnetic white dwarf GD 229," Astrophys. J. **463**, 320 (1996).

[41] G. D. Schmidt, R. G. Allen, P. S. Smith, and J. Liebert, "Erratum: 'Combined ultraviolet-optical spectropolarimetry of the magnetic white dwarf GD 229' (ApJ, 463, 320 [1996])," Astrophys. J. **473**, 569 (1996).

[42] P. Dufour, J. Liebert, G. Fontaine, and N. Behara, "White dwarf stars with carbon atmospheres," Nature **450**, 522–524 (2007).

[43] A. Kawka, S. Vennes, L. Ferrario, and E. Paunzen, "Evidence of enhanced magnetism in cool, polluted white dwarfs," Mon. Not. R. Astron. Soc. **482**, 5201–5210 (2019).

[44]S. V. Berdyugina, A. V. Berdyugin, and V. Piirola, "Molecular magnetic dichroism in spectra of white dwarfs," Phys. Rev. Lett. **99**, 091101 (2007).
[45]J. J. Dongarra, J. Du Croz, S. Hammarling, and I. S. Duff, "A set of level 3 basic linear algebra subprograms," ACM Trans. Math. Software **16**, 1–17 (1990).
[46]F. London, "Théorie quantique des courants interatomiques dans les combinaisons aromatiques," J. Phys. Radium **8**, 397–409 (1937).
[47]F. Hampe, S. Stopkowicz, N. Groß, M.-P. Kitsaras, L. Grazioli, S. Blaschke, L. Monzel, and Ü. P. Yergün, "QCUMBRE, quantum chemical utility enabling magnetic-field dependent investigations benefitting from rigorous electron-correlation treatment," Qcumbre.org.
[48]J. F. Stanton, J. Gauss, L. Cheng, M. E. Harding, D. A. Matthews, and P. G. Szalay, "CFOUR, coupled-cluster techniques for computational chemistry, a quantum-chemical program package," with contributions from A. Asthana, A. A. Auer, R. J. Bartlett, U. Benedikt, C. Berger, D. E. Bernholdt, S. Blaschke, Y. J. Bomble, S. Burger, O. Christiansen, D. Datta, F. Engel, R. Faber, J. Greiner, M. Heckert, O. Heun, M. Hilgenberg, C. Huber, T.-C. Jagau, D. Jonsson, J. Jusélius, T. Kirsch, M.-P. Kitsaras, K. Klein, G. M. Kopper, W. J. Lauderdale, F. Lipparini, J. Liu, T. Metzroth, L. A. Mück, D. P. O'Neill, T. Nottoli, J. Oswald, D. R. Price, E. Prochnow, C. Puzzarini, K. Ruud, F. Schiffmann, W. Schwalbach, C. Simmons, S. Stopkowicz, A. Tajti, T. Uhlirova, J. Vázquez, F. Wang, J. D. Watts, P. Yergün, C. Zhang, and X. Zheng, and the integral packages MOLECULE (J. Almlöf and P. R. Taylor), PROPS (P. R. Taylor), ABACUS (T. Helgaker, H. J. A. Jensen, P. Jørgensen, and J. Olsen), and ECP routines by A. V. Mitin and C. van Wüllen, for the current version, see http://www.cfour.de.
[49]E. Tellgren, T. Helgaker, A. Soncini, K. K. Lange, A. M. Teale, U. Ekström, S. Stopkowicz, J. H. Austad, and S. Sen, "LONDON, a quantum-chemistry program for plane-wave/GTO hybrid basis sets and finite magnetic field calculations," londonprogram.org.
[50]QUEST, A rapid development platform for QUantum Electronic Structure Techniques, 2017, quest.codes.
[51]BAGEL, Brilliantly Advanced General Electronic-structure Library, http://www.nubakery.org under the GNU General Public License.
[52]D. B. Williams-Young, A. Petrone, S. Sun, T. F. Stetina, P. Lestrange, C. E. Hoyer, D. R. Nascimento, L. Koulias, A. Wildman, J. Kasper, J. J. Goings, F. Ding, A. E. DePrince, E. F. Valeev, and X. Li, "The Chronus Quantum software package," Wiley Interdiscip. Rev.: Comput. Mol. Sci. **10**, e1436 (2020).
[53]Y. J. Franzke, C. Holzer, J. H. Andersen, T. Begušić, F. Bruder, S. Coriani, F. Della Sala, E. Fabiano, D. A. Fedotov, S. Fürst, S. Gillhuber, R. Grotjahn, M. Kaupp, M. Kehry, M. Krstić, F. Mack, S. Majumdar, B. D. Nguyen, S. M. Parker, F. Pauly, A. Pausch, E. Perlt, G. S. Phun, A. Rajabi, D. Rappoport, B. Samal, T. Schrader, M. Sharma, E. Tapavicza, R. S. Treß, V. Voora, A. Wodyński, J. M. Yu, B. Zerulla, F. Furche, C. Hättig, M. Sierka, D. P. Tew, and F. Weigend, "TURBOMOLE: Today and tomorrow," J. Chem. Theory Comput. **19**, 6859–6890 (2023).
[54]F. A. Bischoff, "Structure of the H_3 molecule in a strong homogeneous magnetic field as computed by the Hartree-Fock method using multiresolution analysis," Phys. Rev. A **101**, 053413 (2020).
[55]J. Čížek, "On the correlation problem in atomic and molecular systems. Calculation of wavefunction components in Ursell-type expansion using quantum-field theoretical methods," J. Chem. Phys. **45**, 4256–4266 (1966).
[56]H. J. Monkhorst, "Calculation of properties with the coupled-cluster method," Int. J. Quantum Chem. **12**, 421–432 (1977).
[57]F. Hampe and S. Stopkowicz, "Transition-dipole moments for electronic excitations in strong magnetic fields using equation-of-motion and linear response coupled-cluster theory," J. Chem. Theory Comput. **15**, 4036–4043 (2019).
[58]F. Hampe, N. Gross, and S. Stopkowicz, "Full triples contribution in coupled-cluster and equation-of-motion coupled-cluster methods for atoms and molecules in strong magnetic fields," Phys. Chem. Chem. Phys. **22**, 23522–23529 (2020).
[59]I. Shavitt and R. J. Bartlett, *Many-Body Methods in Chemistry and Physics: MBPT and Coupled-Cluster Theory* (Cambridge University Press, Cambridge, 2009).
[60]D. M. Bishop, *Group Theory and Chemistry* (Dover Publications, 1973).
[61]E. R. Davidson, "Use of double cosets in constructing integrals over symmetry orbitals," J. Chem. Phys. **62**, 400 (1975).
[62]P. R. Taylor, "Symmetry-adapted integral derivatives," Theor. Chim. Acta **69**, 447–460 (1986).
[63]A. Pausch, M. Gebele, and W. Klopper, "Molecular point groups and symmetry in external magnetic fields," J. Chem. Phys. **155**, 201101 (2021).
[64]M.-P. Kitsaras and S. Stopkowicz, "Exploiting symmetry in quantum-chemical calculations in finite magnetic field: Abelian complex groups" (unpublished) (2024).
[65]M.-P. Kitsaras, "Finite magnetic-field coupled-cluster methods: Efficiency and utilities," Ph.D. thesis, Johannes-Gutenberg Universität Mainz, 2023.
[66]E. Epifanovsky, D. Zuev, X. Feng, K. Khistyaev, Y. Shao, and A. I. Krylov, "General implementation of the resolution-of-the-identity and Cholesky representations of electron repulsion integrals within coupled-cluster and equation-of-motion methods: Theory and benchmarks," J. Chem. Phys. **139**, 134105 (2013).
[67]S. D. Folkestad, E. F. Kjønstad, and H. Koch, "An efficient algorithm for Cholesky decomposition of electron repulsion integrals," J. Chem. Phys. **150**, 194112 (2019).
[68]J. Gauss, S. Blaschke, S. Burger, T. Nottoli, F. Lipparini, and S. Stopkowicz, "Cholesky decomposition of two-electron integrals in quantum-chemical calculations with perturbative or finite magnetic fields using gauge-including atomic orbitals," Mol. Phys. **121**, e2101562 (2023).
[69]R. D. Reynolds and T. Shiozaki, "Fully relativistic self-consistent field under a magnetic field," Phys. Chem. Chem. Phys. **17**, 14280–14283 (2015).
[70]O. Christiansen, H. Koch, and P. Jørgensen, "The second-order approximate coupled cluster singles and doubles model CC2," Chem. Phys. Lett. **243**, 409–418 (1995).
[71]O. Christiansen, H. Koch, and P. Jørgensen, "Response functions in the CC3 iterative triple excitation model," J. Chem. Phys. **103**, 7429–7441 (1995).
[72]H. Koch, O. Christiansen, P. Jørgensen, A. M. Sanchez de Merás, and T. Helgaker, "The CC3 model: An iterative coupled cluster approach including connected triples," J. Chem. Phys. **106**, 1808–1818 (1997).
[73]A. C. Paul, R. H. Myhre, and H. Koch, "New and efficient implementation of CC3," J. Chem. Theory Comput. **17**, 117–126 (2021); arXiv:2007.01088.
[74]C. Wiebeler, J. Vollbrecht, A. Neuba, H.-S. Kitzerow, and S. Schumacher, "Unraveling the electrochemical and spectroscopic properties of neutral and negatively charged perylene tetraethylesters," Sci. Rep. **11**, 16097 (2021).
[75]M. H. Stockett, C. Kjær, S. Daly, E. J. Bieske, J. R. R. Verlet, S. B. Nielsen, and J. N. Bull, "Photophysics of isolated rose bengal anions," J. Phys. Chem. A **124**, 8429–8438 (2020).
[76]M. Hornum, P. Reinholdt, J. K. Zaręba, B. B. Jensen, D. Wüstner, M. Samoć, P. Nielsen, and J. Kongsted, "One- and two-photon solvatochromism of the fluorescent dye Nile Red and its CF3, F and Br-substituted analogues," Photochem. Photobiol. Sci. **19**, 1382–1391 (2020).
[77]M.-S. Dupuy, E. Gloaguen, B. Tardivel, M. Mons, and V. Brenner, "CC2 benchmark for models of phenylalanine protein chains: 0–0 transition energies and IR signatures of the $\pi\pi^*$ excited state," J. Chem. Theory Comput. **16**, 601–611 (2020).
[78]B. Durbeej, "Competing excited-state deactivation processes in bacteriophytochromes," Adv. Quantum Chem. **81**, 243–268 (2020).
[79]X. F. Yu, T. H. Fu, B. Xiao, H. Y. Yu, and Q. Li, "A theoretical study on the excited-state deactivation paths for the A–5FU dimer," Phys. Chem. Chem. Phys. **23**, 16089–16106 (2021).
[80]P. Reinholdt, M. L. Vidal, J. Kongsted, M. Iannuzzi, S. Coriani, and M. Odelius, "Nitrogen *K*-edge x-ray absorption spectra of ammonium and ammonia in water solution: Assessing the performance of polarizable embedding coupled cluster methods," J. Phys. Chem. Lett. **12**, 8865–8871 (2021).
[81]D. A. Safin, M. G. Babashkina, M. Bolte, A. L. Ptaszek, M. Kukułka, and M. P. Mitoraj, "Novel sterically demanding Schiff base dyes: An insight from experimental and theoretical calculations," J. Lumin. **238**, 118264 (2021).
[82]M. A. Kochman, B. Durbeej, and A. Kubas, "Simulation and analysis of the transient absorption spectrum of 4-(N,N-dimethylamino)benzonitrile (DMABN) in acetonitrile," J. Phys. Chem. A **125**, 8635–8648 (2021).
[83]C. Naim, F. Castet, and E. Matito, "Impact of van der Waals interactions on the structural and nonlinear optical properties of azobenzene switches," Phys. Chem. Chem. Phys. **23**, 21227–21239 (2021).
[84]R. Izsák, "Single-reference coupled cluster methods for computing excitation energies in large molecules: The efficiency and accuracy of approximations," Wiley Interdiscip. Rev.: Comput. Mol. Sci. **10**, e1445 (2020).

[85]C. Hättig, "Beyond Hartree-Fock: MP2 and coupled-cluster methods for large systems," in *Computational Nanoscience: Do It Yourself!*, edited by J. Grotendorst, S. Blügel, and D. Marx (John von Neumann Institute for Computing, 2006), Vol. 31, pp. 245–278.
[86]M. Schreiber, M. R. Silva-Junior, S. P. A. Sauer, and W. Thiel, "Benchmarks for electronically excited states: CASPT2, CC2, CCSD, and CC3," J. Chem. Phys. **128**, 134110 (2008).
[87]M.-P. Kitsaras and S. Stopkowicz, "Spin contamination in MP2 and CC2, a surprising issue," J. Chem. Phys. **154**, 131101 (2021).
[88]G. D. Purvis and R. J. Bartlett, "A full coupled-cluster singles and doubles model: The inclusion of disconnected triples," J. Chem. Phys. **76**, 1910–1918 (1982).
[89]A. I. Krylov, "The quantum chemistry of open-shell species," in *Reviews in Computational Chemistry*, edited by A. L. Parrill and K. B. Lipkowitz (John Wiley & Sons, Ltd., 2017), pp. 151–224.
[90]M. Bondanza, D. Jacquemin, and B. Mennucci, "Excited states of xanthophylls revisited: Toward the simulation of biologically relevant systems," J. Phys. Chem. Lett. **12**, 6604–6612 (2021).
[91]T. J. A. Wolf, R. H. Myhre, J. P. Cryan, S. Coriani, R. J. Squibb, A. Battistoni, N. Berrah, C. Bostedt, P. Bucksbaum, G. Coslovich, R. Feifel, K. J. Gaffney, J. Grilj, T. J. Martinez, S. Miyabe, S. P. Moeller, M. Mucke, A. Natan, R. Obaid, T. Osipov, O. Plekan, S. Wang, H. Koch, and M. Gühr, "Probing ultrafast $\pi\pi^*/n\pi^*$ internal conversion in organic chromophores via K-edge resonant absorption," Nat. Commun. **8**, 29 (2017).
[92]J. P. Carbone, L. Cheng, R. H. Myhre, D. Matthews, H. Koch, and S. Coriani, "Chapter eleven—An analysis of the performance of coupled cluster methods for k-edge core excitations and ionizations using standard basis sets," in *State of the Art of Molecular Electronic Structure Computations: Correlation Methods, Basis Sets and More*, *Advances in Quantum Chemistry*, edited by L. U. Ancarani and P. E. Hoggan (Academic Press, 2019), Vol. 79, pp. 241–261.
[93]M. C. Davis and R. C. Fortenberry, "(T)+EOM quartic force fields for theoretical vibrational spectroscopy of electronically excited states," J. Chem. Theory Comput. **17**, 4374–4382 (2021).
[94]G. Bilalbegović, A. Maksimović, L. A. Valencic, and S. Lehtola, "Sulfur molecules in space by x-rays: A computational study," ACS Earth Space Chem. **5**, 436–448 (2021).
[95]A. Hutcheson, A. C. Paul, R. H. Myhre, H. Koch, and I. Høyvik, "Describing ground and excited state potential energy surfaces for molecular photoswitches using coupled cluster models," J. Comput. Chem. **42**, 1419–1429 (2021).
[96]S. P. Neville, A. Stolow, and M. S. Schuurman, "Vacuum ultraviolet excited state dynamics of the smallest ring, cyclopropane. I. A reinterpretation of the electronic spectrum and the effect of intensity borrowing," J. Chem. Phys. **149**, 144310 (2018).
[97]D. A. Fedotov, A. C. Paul, P. Posocco, F. Santoro, M. Garavelli, H. Koch, S. Coriani, and R. Improta, "Excited-state absorption of uracil in the gas phase: Mapping the main decay paths by different electronic structure methods," J. Chem. Theory Comput. **17**, 1638–1652 (2021).
[98]M. Véril, A. Scemama, M. Caffarel, F. Lipparini, M. Boggio-Pasqua, D. Jacquemin, and P. Loos, "QUESTDB: A database of highly accurate excitation energies for the electronic structure community," Wiley Interdiscip. Rev.: Comput. Mol. Sci. **11**, e1517 (2021).
[99]D. A. Matthews, "EOM-CC methods with approximate triple excitations applied to core excitation and ionisation energies," Mol. Phys. **118**, e1771448 (2020).
[100]P.-F. Loos, F. Lipparini, M. Boggio-Pasqua, A. Scemama, and D. Jacquemin, "A mountaineering strategy to excited states: Highly accurate energies and benchmarks for medium sized molecules," J. Chem. Theory Comput. **16**, 1711–1741 (2020).
[101]A. Köhn and A. Tajti, "Can coupled-cluster theory treat conical intersections?," J. Chem. Phys. **127**, 044105 (2007).
[102]S. Thomas, F. Hampe, S. Stopkowicz, and J. Gauss, "Complex ground-state and excitation energies in coupled-cluster theory," Mol. Phys. **119**, e1968056 (2021); arXiv:2106.03757.
[103]J. Liu, A. Asthana, L. Cheng, and D. Mukherjee, "Unitary coupled-cluster based self-consistent polarization propagator theory: A third-order formulation and pilot applications," J. Chem. Phys. **148**, 244110 (2018).
[104]M. Hodecker, D. R. Rehn, and A. Dreuw, "Hermitian second-order methods for excited electronic states: Unitary coupled cluster in comparison with algebraic–diagrammatic construction schemes," J. Chem. Phys. **152**, 094106 (2020).
[105]L. Grazioli and S. Stopkowicz, "Unitary coupled-cluster theory for the treatment of molecules in strong magnetic fields" (unpublished) (2024).
[106]C. Møller and M. S. Plesset, "Note on an approximation treatment for many-electron systems," Phys. Rev. **46**, 618–622 (1934).
[107]B. Helmich-Paris, C. Hättig, and C. van Wüllen, "Spin-free CC2 implementation of induced transitions between singlet ground and triplet excited states," J. Chem. Theory Comput. **12**, 1892–1904 (2016).
[108]D. A. Matthews, L. Cheng, M. E. Harding, F. Lipparini, S. Stopkowicz, T.-C. Jagau, P. G. Szalay, J. Gauss, and J. F. Stanton, "Coupled-cluster techniques for computational chemistry: The CFOUR program package," J. Chem. Phys. **152**, 214108 (2020).
[109]J. Gauss, F. Lipparini, S. Burger, S. Blaschke, M.-P. Kitsaras, T. Nottoli, J. Oswald, and S. Stopkowicz, "MINT, Mainz INTegral package," Johannes Gutenberg-Universität Mainz, 2015–2023.
[110]B. Zuckerman, D. Koester, I. N. Reid, and M. Hunsch, "Metal lines in DA white dwarfs," Astrophys. J. **596**, 477–495 (2003).
[111]B. Zuckerman, C. Melis, B. Klein, D. Koester, and M. Jura, "Ancient planetary systems are orbiting a large fraction of white dwarf stars," Astrophys. J. **722**, 725–736 (2010).
[112]A. Kramida, Y. Ralchenko, and J. Reader, and NIST ASD Team, NIST Atomic Spectra Database, National Institute of Standards and Technology, Gaithersburg, MD, 2022, https://physics.nist.gov/asd.
[113]B. P. Pritchard, D. Altarawy, B. Didier, T. D. Gibson, and T. L. Windus, "New basis set exchange: An open, up-to-date resource for the molecular sciences community," J. Chem. Inf. Model. **59**, 4814–4820 (2019).
[114]D. Feller, "The role of databases in support of computational chemistry calculations," J. Comput. Chem. **17**, 1571–1586 (1996).
[115]K. L. Schuchardt, B. T. Didier, T. Elsethagen, L. Sun, V. Gurumoorthi, J. Chase, J. Li, and T. L. Windus, "Basis set exchange: A community database for computational sciences," J. Chem. Inf. Model. **47**, 1045–1052 (2007).
[116]B. P. Prascher, D. E. Woon, K. A. Peterson, T. H. Dunning, and A. K. Wilson, "Gaussian basis sets for use in correlated molecular calculations. VII. Valence, core-valence, and scalar relativistic basis sets for Li, Be, Na, and Mg," Theor. Chem. Acc. **128**, 69–82 (2011).
[117]The first label of the electronic state corresponds to the multiplicity and irreducible representation of the state in magnetic field, while the second label in parenthesis refers to the corresponding state in zero field.
[118]M. A. Hollands, S. Stopkowicz, M.-P. Kitsaras, F. Hampe, S. Blaschke, and J. J. Hermes, "A DZ white dwarf with a 30 MG magnetic field," Mon. Not. R. Astron. Soc. **520**, 3560–3575 (2023).
[119]M. J. Pemberton, T. J. P. Irons, T. Helgaker, and A. M. Teale, "Revealing the exotic structure of molecules in strong magnetic fields," J. Chem. Phys. **156**, 204113 (2022).